An Experimental Comparison of Several PWM Controllers for a Single-Phase AC–DC Converter

D. Karagiannis*, E. Mendes♯, A. Astolfi*◇, R. Ortega♮

*Department of Electrical and Electronic Engineering
Imperial College, London, SW7 2BT, United Kingdom
{d.karagiannis,a.astolfi}@ic.ac.uk,

♯Laboratoire de Génie Electrique de Paris
CNRS-SUPELEC, 91192 Gif-sur-Yvette, France
mendes@lgep.supelec.fr,

◇Dipartimento di Elettronica e Informazione
Politecnico di Milano, 20133 Milano, Italy

♮Laboratoire des Signaux et Systèmes
CNRS-SUPELEC, 91190 Gif-sur-Yvette, France
Romeo.Ortega@lss.supelec.fr,

Abstract

An experimental comparative study of various controllers for a class of AC–DC converters, known as *power factor precompensators*, is presented. The control objective is to robustly regulate the output voltage to a desired constant level in the presence of variations in the load, while retaining a unit power factor at the input, *i.e.* the input current should follow in frequency and in phase the input voltage. Several control schemes are presented and compared via experiments.

Keywords: AC–DC power conversion, adaptive control, pulse width modulation, reactive power compensation.

1 Introduction

Power factor precompensators (PFP) are an important class of switched AC–DC converters. As their name suggests, their main function is to achieve a nearly unit power factor by drawing a sinusoidal current that is in phase with the source voltage, thus eliminating the reactive power and the harmonic interference with other equipment operating off the same source.

More precisely, the control objective is twofold. First, the input current should track a sinusoidal reference signal that is in phase with the input voltage. Second, the output voltage should be driven to a desired constant level. An additional requirement is robustness against variation of the system parameters and in particular of the load, which is usually unknown.

As the amplitude of the input current determines explicitly the DC output voltage, one may satisfy both objectives in a single *current control* loop, which typically comprises a hysteresis or sliding mode controller (see [4, Chapter 18] for a general description and [5] for a design example).

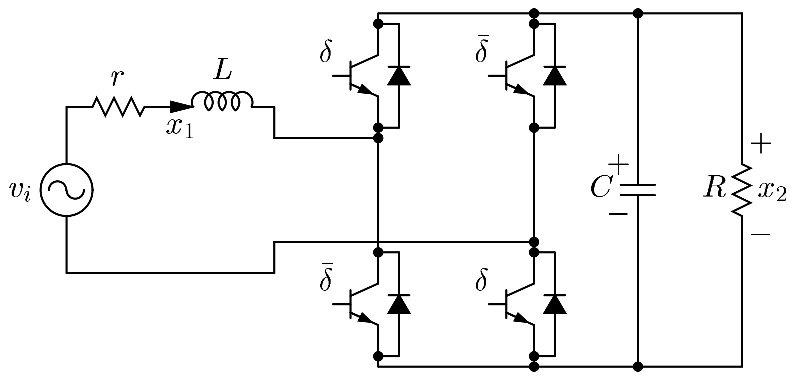

Figure 1: The full-bridge boost PFP circuit.

The main drawback of these controllers is that they require very high switching frequency (typically few hundred kHz) leading to high converter losses. In this work, we are interested in pulse-width modulation (PWM) control techniques, which are based on *averaged models* [3] and can be implemented using lower switching frequency (*e.g.* 10kHz). Furthermore, the issue of robustness against variations of the load is treated by appropriate adaptive schemes. This allows to avoid the use of an output current sensor, thus making the practical implementation more attractive.

The paper is organised as follows. In Section 2, we analyse the model of the PFP, define the desired equilibrium regime and specify the control strategy. In Section 3, we propose various control schemes that achieve the control objectives. An adaptive version for each controller is considered separately. In Section 4, we present the experimental results and compare the performance of the proposed controllers. Conclusions are given in Section 5.

2 The PFP circuit

We consider the *full-bridge boost* PFP circuit shown in Figure 1, which consists of two pairs of transistor-diode switches working in a complementary way. The switching signal δ is generated by a PWM circuit and takes values in the finite set $\{-1, 1\}$. The averaged model of the PFP can be obtained using Kirchhoff's laws and is given by the equations

$$L\dot{x}_1 = -ux_2 - rx_1 + v_i(t) \tag{1}$$

$$C\dot{x}_2 = ux_1 - \frac{1}{R}x_2, \tag{2}$$

where $v_i(t) = Esin(\omega t)$ is the source voltage, x_1 is the input (inductor) current, $x_2 > 0$ is the output (capacitor) voltage and $u \in [-1, 1]$ is the duty ratio of the PWM.[1]

The desired input current in steady-state is

$$x_1^\star(t) = I_d \sin(\omega t), \tag{3}$$

for some $I_d > 0$ yet to be specified. Substituting equation (3) into equation (1) yields the steady-state value for ux_2, namely

$$u^\star(t)x_2^\star(t) = v_i(t) - rx_1^\star(t) - L\dot{x}_1^\star(t). \tag{4}$$

[1] Note that the exact model of the PFP is described by the same equations, if we replace u with δ.

Substituting equations (3) and (4) into equation (2) written for $x_2 = x_2^\star$ yields

$$C\dot{x}_2^\star x_2^\star = -\frac{1}{R}x_2^{\star 2} + \frac{(E - rI_d)I_d}{2} - \frac{(E - rI_d)I_d}{2}\cos(2wt) - \frac{LI_d^2 w}{2}\sin(2wt). \tag{5}$$

The steady-state solution of (5) can be directly computed and is given by

$$x_2^{\star 2}(t) = \frac{(E - rI_d)RI_d}{2} + A\sin(2\omega t + \phi), \tag{6}$$

where

$$A = \frac{RI_d}{2}\sqrt{\frac{(LI_d\omega)^2 + (E - rI_d)^2}{1 + (RC\omega)^2}},$$

$$\phi = \arctan\frac{E - rI_d - RC\omega LI_d\omega}{LI_d\omega + RC\omega(E - rI_d)}.$$

Hence, in steady-state, $x_2^{\star 2}(t)$ consists only of a DC term and a second-order harmonic, which can be neglected, since in practice its amplitude is much smaller than the DC term. The average of $x_2(t)$, denoted by V_d, is given by

$$V_d = \sqrt{\frac{(E - rI_d)RI_d}{2}}. \tag{7}$$

From (7), solving for I_d yields the solutions

$$I_d = \frac{E}{2r} \pm \sqrt{\frac{E^2}{4r^2} - \frac{2V_d^2}{rR}},$$

which are real if and only if

$$\frac{V_d}{E} \le \sqrt{\frac{R}{8r}}.$$

Selecting the smallest solution, which corresponds to minimum power (*i.e.* minimum converter losses), the amplitude of the input current that drives the output voltage to the desired level V_d is given by

$$I_d = \frac{E}{2r} - \sqrt{\frac{E^2}{4r^2} - \frac{2V_d^2}{rR}}. \tag{8}$$

Note that the same solution has been obtained by a similar analysis in [2].

We conclude that by controlling the input current so that it tracks the signal (3), where I_d is given by equation (8), we can achieve both control objectives, namely unit power factor and output voltage regulation, provided that the closed-loop system is asymptotically stable.

The main drawback of this approach, as equations (7) and (8) reveal, is the sensitivity of the output voltage to the parameters r and R. The dependence on R poses a significant problem, since in many applications the load is unknown or time-varying. This obstacle can be overcome by adding an adaptation scheme either on I_d or on R.

Remark 1 Recall that the control signal u must satisfy the constraint $|u| \le 1$. A necessary condition for the existence of this control is derived in [2] and shows that the PFP can only work as a boost converter.

3 Control laws

In this section, we propose four controllers for the regulation of the input current. First, we consider the case where all the parameters are known, so we can use equation (8) to compute the reference current. An adaptive scheme will later be added to deal with the uncertainty in the load.

3.1 The known parameter case

The control designs that will be compared are the following.

A. Passivity-Based (PB)

In [2], the passivity-based controller described by the equation

$$u = \frac{1}{x_{2d}}\left[v_i - rx_1 - L\dot{x}_1^\star - K_1(x_1^\star - x_1)\right], \tag{9}$$

where the auxiliary variable $x_{2d} > 0$ is the solution of

$$C\dot{x}_{2d} = ux_1^\star - \frac{1}{R}x_{2d} - K_2(x_{2d} - x_2) \tag{10}$$

with $x_1^\star$ given by (3) has been proposed. This controller renders the closed-loop system passive with the storage function

$$H = \frac{L}{2}(x_1^\star - x_1)^2 + \frac{C}{2}(x_{2d} - x_2)^2,$$

whose time derivative is given by

$$\begin{aligned} \dot{H} &= -K_1(x_1^\star - x_1)^2 - (R^{-1} + K_2)(x_{2d} - x_2)^2 \\ &\leq -2\frac{\min\left(K_1, R^{-1} + K_2\right)}{\max\left(L, C\right)}H. \end{aligned}$$

Hence, for $K_1 > 0$ and $K_2 > 0$, x_1, x_2 converge exponentially to $x_1^\star$, x_{2d} respectively. Moreover, the average of x_{2d} converges to V_d provided that equation (8) holds.

B. Feed-Forward (FF)

If we replace in the control law (9) the auxiliary state x_{2d} with the output voltage x_2, we obtain the simplified controller

$$u = \frac{1}{x_2}\left[v_i - rx_1^\star - L\dot{x}_1^\star - K_1(x_1^\star - x_1)\right]. \tag{11}$$

Substituting equation (11) into equation (1) and defining $\tilde{x}_1 = x_1^\star - x_1$ yields the *linearised* error dynamics

$$L\dot{\tilde{x}}_1 = -(r + K_1)\tilde{x}_1,$$

which is exponentially stable for any $K_1 > -r$. Hence, the time response of x_1 is given by

$$x_1(t) = x_1(0)\exp\left(-\frac{r + K_1}{L}t\right) + I_d\sin(\omega t). \tag{12}$$

Assuming that x_1 takes its steady-state value $x_1(t) = I_d \sin(\omega t)$ immediately and substituting into equation (2) yields

$$\dot{x}_2 = -\frac{1}{RC}x_2 + \frac{E - rI_d}{2Cx_2}I_d - \frac{E - rI_d}{2Cx_2}I_d\cos(2\omega t) - \frac{LI_d^2\omega}{2Cx_2}\sin(2\omega t). \tag{13}$$

Rewriting equation (13) in the variable x_2^2 yields the *linear* dynamics

$$\dot{x}_2^2 = -\frac{2}{RC}x_2^2 + \frac{E - rI_d}{C}I_d - \frac{E - rI_d}{C}I_d\cos(2\omega t) - \frac{LI_d^2\omega}{C}\sin(2\omega t), \tag{14}$$

showing that x_2 converges (in average) to the desired voltage.

Remark 2 The FF controller is actually a feedback linearising controller. The term "feed-forward" arises from the use of $x_1^\star$ and $\dot{x}_1^\star$ in the control law (11).

C. Feedback Linearisation (FL)

A static feedback control law that linearises the input-output behaviour of the system with output the inductor current is described by the equation

$$u = \frac{1}{x_2}[v_i - rx_1 - w]. \tag{15}$$

It is easy to see that the resulting linearised system with input w and output x_1 is an integrator. Thus, if we apply proportional control, *i.e.*

$$w = K_1(x_1^\star - x_1) \tag{16}$$

with $K_1 > 0$, then it can be shown that the closed-loop system is asymptotically stable. The closed-loop dynamics of x_1 are given by

$$L\dot{x}_1 = -K_1x_1 + K_1I_d\sin(\omega t),$$

hence, in steady-state,

$$x_1(t) = \frac{1}{\sqrt{1+\mu^2}}I_d\sin(\omega t - \arctan\mu), \tag{17}$$

where $\mu = L\omega/K_1$. As a result, in this case, there is a steady-state error,[2] which decreases as we increase the gain K_1. Note, finally, that if K_1 is selected sufficiently large, x_2 converges to the desired voltage.

D. Internal Model (IM)

If instead of x_1 we take as output the signal $z = ux_2$, which corresponds to the input voltage of the transistor-diode bridge, then the system can be linearised by means of the dynamic controller[3]

$$\dot{u} = \frac{1}{x_2}\left(-\frac{u^2x_1}{C} + w\right). \tag{18}$$

[2] In particular, there is a negative phase-shift, *i.e.* the input current leads the input voltage.

[3] To prove this fact, consider the dynamics of z: $\dot{z} = \dot{u}x_2 + \frac{u^2x_1}{C} - \frac{1}{RC}z$.

The linearised system is described by the equations

$$\begin{bmatrix} \dot{x}_1 \\ \dot{z} \end{bmatrix} = \begin{bmatrix} -r/L & -1/L \\ 0 & -1/RC \end{bmatrix} \begin{bmatrix} x_1 \\ z \end{bmatrix} + \begin{bmatrix} 1 & 0 \\ 0 & 1 \end{bmatrix} \begin{bmatrix} v_i/L \\ w \end{bmatrix}, \tag{19}$$

$$y = \begin{bmatrix} 0 & 1 \end{bmatrix} \begin{bmatrix} x_1 \\ z \end{bmatrix}. \tag{20}$$

Hence, the transfer function from w to y is given by[4]

$$G(s) = \frac{1}{s + 1/RC}. \tag{21}$$

It is clear from the analysis in Section 2 that we can achieve the control objectives by forcing $y(t)$ to track the signal

$$y^\star(t) = z^\star(t) = v_i - r x_1^\star - L\dot{x}_1^\star. \tag{22}$$

To this end, consider the error

$$e = y^\star - y = v_i - r x_1^\star - L\dot{x}_1^\star - u x_2 \tag{23}$$

and the controller

$$K(s) = \frac{w(s)}{e(s)} = k\frac{s^2 + as + b}{s^2 + \omega^2}, \tag{24}$$

where $k > 0$, $a > 0$ and $b > 0$ are design parameters. Then, for sufficiently large k, the closed-loop system is asymptotically stable. Moreover, by the presence of the poles at $s = \pm j\omega$, we conclude that z converges to $z^\star$ and hence x_1 converges to $x_1^\star$.

Remark 3 The choice of the controller (24) is motivated by the internal model principle and the fact that the reference signal $y^\star(t)$ is a sinusoid of frequency ω. Furthermore, the zeros have been inserted to ensure stability.

Remark 4 In practice, in order to compensate for unmodeled dynamics, it is necessary to add to the reference signal (22) a correction term proportional to the error $\tilde{x}_1 = x_1^\star - x_1$, *i.e.*

$$z^\star(t) = v_i - r x_1^\star - L\dot{x}_1^\star - K_1(x_1^\star - x_1).$$

To incorporate this into our linear formulation, consider instead of (20) the output

$$y(t) = \begin{bmatrix} -K_1 & 1 \end{bmatrix} \begin{bmatrix} x_1(t) \\ z(t) \end{bmatrix}$$

and the reference

$$y^\star(t) = v_i - r x_1^\star - L\dot{x}_1^\star - K_1 x_1^\star.$$

The transfer function from w to y is now given by

$$G(s) = \frac{s + (r + K_1)/L}{(s + r/L)(s + 1/RC)}. \tag{25}$$

Clearly, for sufficiently large $k > 0$, the closed-loop system is asymptotically stable provided that $K_1 > -r$.

[4] Note the cancellation of the stable pole at $s = -r/L$.

3.2 The unknown parameter case

So far we have assumed that the parameters r and R were known and so we could control the output voltage indirectly via formula (8). In practice, however, the load R is usually unknown or time-varying. To overcome this robustness problem, it is necessary to add an adaptation scheme either to the parameter R or to the parameter I_d.

We describe three adaptation schemes, for which (under some mild assumptions) asymptotic stability can be proven. The first one is an estimator proposed in [2] for the PB controller. The other two are based on the recently developed adaptive control methods of *nonlinear PI* (NLPI) control and *immersion and invariance* (I&I) (see [6, 1] for further details).

a. PB estimator

For the PB controller, a projection estimator for $\theta = 1/R$ has been proposed in [2], namely

$$\dot{\hat{\theta}} = \begin{cases} \gamma x_{2d}(x_{2d} - x_2), & \hat{\theta} \geq \varepsilon > 0 \\ 0, & \hat{\theta} < \varepsilon \end{cases} \tag{26}$$

(where $\hat{\theta}$ denotes the estimate of θ) and has been shown to render the equilibrium $(x_1, x_2) = (x_1^\star, x_{2d})$ asymptotically stable, *assuming* that $r = 0$.

b. NLPI control

Invoking time-separation arguments, we can assume that the dynamics of the output voltage are slow compared to the (closed-loop) dynamics of the input current[5] and hence $x_1 = x_1^\star$ at all times.[6] Furthermore, we assume $r = 0$. Then from (13), ignoring second-order harmonics, the dynamics of x_2 are given by

$$\dot{x}_2 = -\frac{1}{RC}x_2 + \frac{E}{2Cx_2}I_d. \tag{27}$$

Note that the assumption $r = 0$ ensures the above system is affine in the "control" I_d.

The equilibrium $x_2 = x_2^\star$ is rendered asymptotically stable by the dynamic control law

$$\dot{I}_d = \alpha\frac{E}{2x_2}\tilde{x}_2 + \beta\dot{\tilde{x}}_2, \tag{28}$$

where α and β are positive constants. To prove this fact, consider the positive definite function

$$V = \frac{1}{2}C\tilde{x}_2^2 + \frac{1}{2\lambda}\left(\tilde{I}_d + \mu\tilde{x}_2\right)^2,$$

whose time derivative along the trajectories of (27)-(28) is given by

$$\dot{V} = -\left(\frac{1}{R} + \frac{V_d}{Rx_2} + \frac{\mu E}{2x_2}\right)\tilde{x}_2^2,$$

which is negative semi-definite and hence the system (27)-(28) is stable. Moreover, $\dot{V} = 0$ implies that $\tilde{x}_2 = 0$ and so, by LaSalle's invariance principle, the system is asymptotically stable.

[5] We can validate this assumption by comparing the time constants of (12) and (14).

[6] Note that, for this assumption to be valid, the dynamics of I_d must be sufficiently slow.

Remark 5 The difference between the controller (28) and a PI is that here the integral gain is not a constant, but a (nonlinear) function of x_2. In particular, it is proportional to the ratio E/x_2. Approximating this ratio by a constant results in the industry-standard PI controller.

Remark 6 The assumption $r = 0$ in the above designs can be replaced by the assumption $rx_1 = \epsilon \sin(\omega t)$ where ϵ is a positive constant. Then we can incorporate the voltage drop across r into the source voltage by taking

$$v_i(t) = (E - \epsilon) sin(\omega t).$$

Note that this simple modification improves the experimental results significantly.

c. I&I control

Using the adaptive I&I method we can design a parameter estimator for both R and r provided that the system (1)-(2) is bounded-input bounded-state (BIBS) stable. We now prove that the trajectories of (1)-(2) are bounded *for any* u.

Consider the positive definite function

$$V = \frac{L}{2} x_1^2 + \frac{C}{2} x_2^2$$

and its time derivative along the system trajectories, namely

$$\dot{V} = -r x_1^2 + v_i x_1 - \frac{1}{R} x_2^2.$$

By Young's inequality, we have

$$\dot{V} \leq -r x_1^2 + \frac{r}{2} x_1^2 + \frac{1}{2r} v_i^2 - \frac{1}{R} x_2^2,$$

hence

$$\dot{V} \leq -\frac{r}{2} x_1^2 - \frac{1}{R} x_2^2 + \frac{1}{2r} v_i^2,$$

which shows that the trajectories remain bounded provided $r > 0$. Note also that the system (1)-(2) is linearly parameterised with respect to the parameters

$$\theta_1 = r, \quad \theta_2 = \frac{1}{R}.$$

Following the adaptive I&I methodology [1], we define the estimation errors

$$z_1 = \hat{\theta}_1 + \beta_1(x_1) - \theta_1,$$

$$z_2 = \hat{\theta}_2 + \beta_2(x_2) - \theta_2$$

and the update laws

$$\dot{\hat{\theta}}_1 = \frac{1}{L} \frac{\partial \beta_1}{\partial x_1} \left(u x_2 - v_i + x_1 (\hat{\theta}_1 + \beta_1) \right), \tag{29}$$

$$\dot{\hat{\theta}}_2 = \frac{1}{C} \frac{\partial \beta_2}{\partial x_2} \left(-u x_1 + x_2 (\hat{\theta}_2 + \beta_2) \right). \tag{30}$$

The resulting error dynamics are

$$\dot{z}_1 = \frac{\partial \beta_1}{\partial x_1}\frac{x_1}{L} z_1, \quad \dot{z}_2 = \frac{\partial \beta_2}{\partial x_2}\frac{x_2}{C} z_2,$$

hence by choosing

$$\beta_1(x_1) = -\kappa x_1^2 \tag{31}$$

$$\beta_2(x_2) = -\lambda x_2, \tag{32}$$

where κ, λ are positive constants and recalling that $x_2 > 0$ and x_1 is not identically zero, we obtain the asymptotically stable dynamics

$$\dot{z}_1 = -\frac{2\kappa x_1^2}{L} z_1, \quad \dot{z}_2 = -\frac{\lambda x_2}{C} z_2.$$

Hence, $\hat{\theta}_1 + \beta_1(x_1)$ converges to θ_1 and $\hat{\theta}_2 + \beta_2(x_2)$ converges to θ_2.

Remark 7 The main advantage of the I&I method is that it relies only on BIBS stability. In this case, we have seen that the trajectories of (1)-(2) are bounded regardless of the input. Hence, the I&I adaptation can be used in conjuction with any stabilising control law $u(x_1, x_2, r, 1/R)$, which can thus be replaced by $u(x_1, x_2, \hat{\theta}_1 + \beta_1, \hat{\theta}_2 + \beta_2)$, where $\hat{\theta}_1$, $\hat{\theta}_2$ and β_1, β_2 are given by (29)-(30) and (31)-(32) respectively.

4 Experimental results

The control algorithms described in Section 3 have been implemented on an experimental system with the parameters shown in Table 1. A diagram of the experimental setup is given in Figure 2. The current control design parameters are set to $K_1 = 15$, $K_2 = 1$, $k = 4600$, $a = 1200$, $b = 2 \cdot 10^5$. The switching frequency of the PWM is 13kHz. The measurements are filtered using low-pass filters with cut-off frequency 7kHz.

Parameter	Value	Unit
E	150	V
ω	100π	rad/sec
r	2.2	Ω
L	2.13	mH
C	1100	μF
R	87	Ω

Table 1: Parameter values for the PFP circuit.

The experiments aim to exhibit the behaviour of the controllers with respect to step changes in the desired output voltage V_d and also with respect to step changes in the load resistance R.

4.1 The known parameter case

To begin with, we consider the non-adaptive versions of the controllers, *i.e.* the parameters r and R are known and I_d is computed from (8). Figure 3 shows the filtered[7] response to

[7]For the comparative graphs to be legible, the harmonics of the output voltage were removed by a moving average filter.

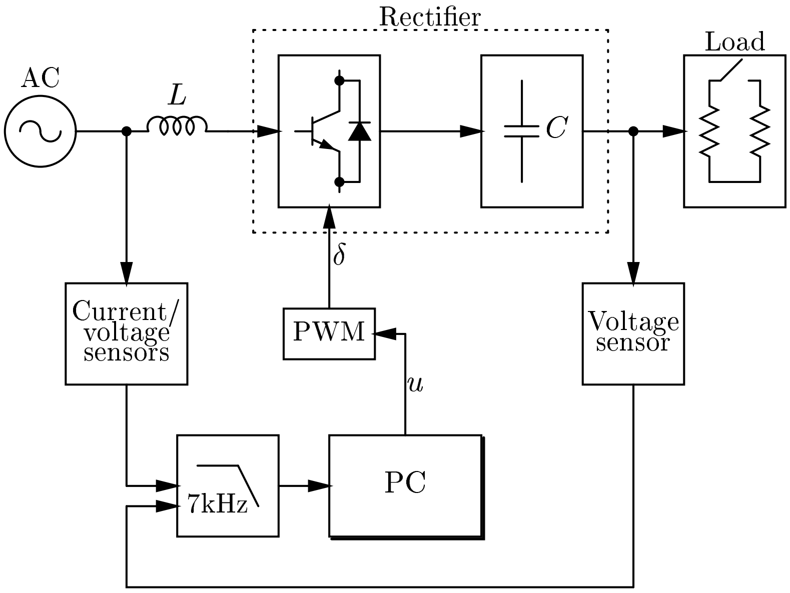

Figure 2: Experimental setup.

an output voltage reference change from 160V to 200V, while Figure 4 shows the harmonic content of the input current for each controller. We see that the transient behaviour of the controllers is almost identical. The PB controller has slightly smaller steady-state error, but larger fourth-order harmonics, owing to the auxiliary dynamics. The steady-state error in all cases is significant, emphasizing the need for parameter adaptation.

Table 2 shows the harmonic characteristics for each controller. We see that the highest power factor and the lowest total harmonic distortion (THD) are achieved by the PB controller. The FL controller achieves the smallest phase shift[8], but with higher THD. On the other hand, the FL controller is the simplest one to implement, since it does not require the derivative of $x_1^\star$ and also it does not depend on the parameters L and C (note, however, that the other control schemes, which depend on L and C are not significantly sensitive to these parameters). Figure 5 shows the input current, output voltage and control input for the FL case.

Control	Error(V)	$\phi(^o)$	THD(%)	Power factor
PB	0.75	1.47	7.53	0.9969
FF	2.59	1.71	7.94	0.9964
FL	1.95	-0.49	8.88	0.9960
IM	2.11	0.68	8.15	0.9966

Table 2: Harmonic analysis results for $R = 87\Omega$.

[8]This is due to the fact that the negative phase shift introduced by FL (see equation (17)) compensates for the positive phase shift of the actual system, which may be caused by unmodeled dynamics and/or time delays.

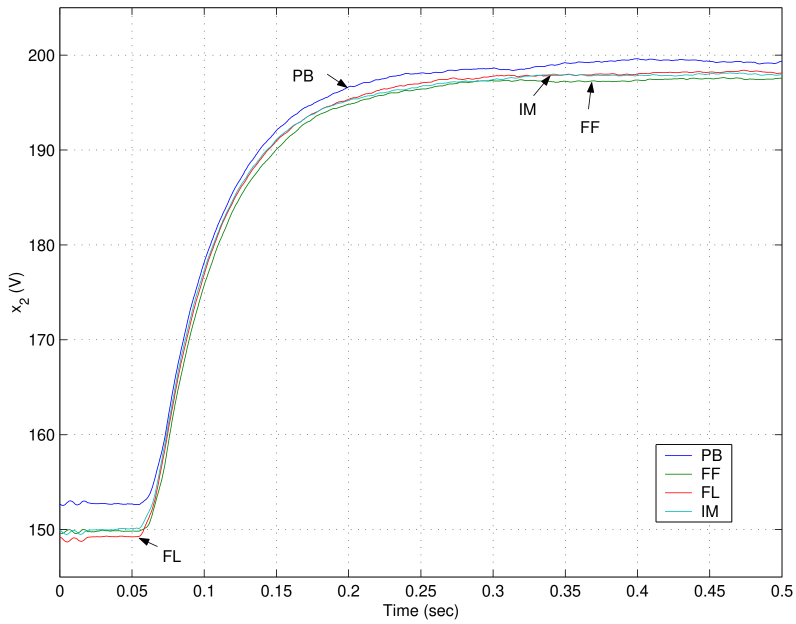

Figure 3: Response of the output voltage to a reference change from 160V to 200V applied at t=0.05s (the known parameter case).

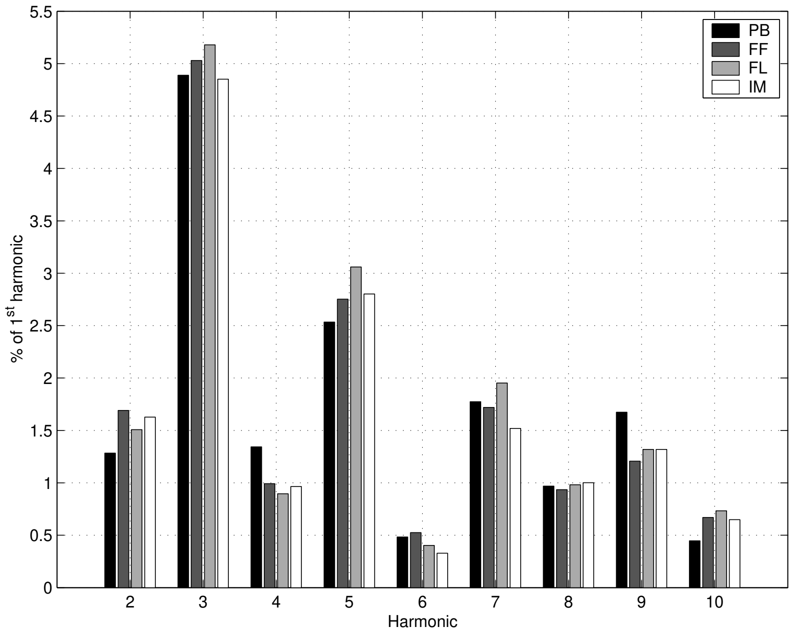

Figure 4: Amplitude of the input current harmonics for $R = 87\Omega$.

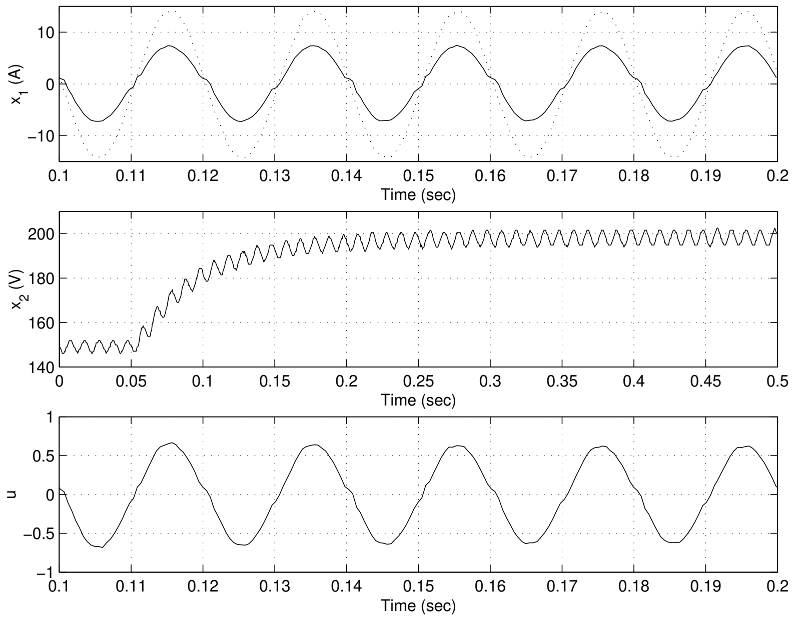

Figure 5: Response to an output voltage reference change for the FL controller. Top graph: input current (solid line) and input voltage (dotted line). Middle graph: output voltage. Bottom graph: control input.

4.2 The unknown parameter case

In this section, we test the controllers *with* the adaptation schemes proposed in Section 3.2. In particular, for the PB controller we apply the PB estimator, while for the FF, FL and IM controllers we employ alternatively the NLPI or the I&I adaptation. The design parameters are given in Table 3. For the sake of comparison, we consider mainly the case (denoted by II_1) where the I&I adaptation is applied only on R (*i.e.* $\kappa = 0$). The full I&I adaptation scheme (denoted by II_2) is considered only with the IM controller.

Adaptation	Parameters
PB	$\gamma = 1 \cdot 10^{-3}$
NLPI	$\alpha = 5, \beta = 0.05$
II_1	$\kappa = 0, \lambda = 2 \cdot 10^{-4}$
II_2	$\kappa = 0.01, \lambda = 2 \cdot 10^{-4}$

Table 3: Parameter values for the PB, NLPI and I&I estimators.

Figure 6 shows the filtered response to a voltage reference change from 160V to 200V. We see that the NLPI control scheme achieves the smallest steady-state error (owing to the integral action), but with a large overshoot. Moreover, experiments have shown that we cannot eliminate this overshoot without degrading the performance of the adaptation significantly. On the other hand, the PB and I&I estimators do not affect the response, which evolves as in the known parameter case.

Figure 7 shows the filtered response to a load change from 87Ω to 51Ω, while Figure 8 shows the harmonic content of the input current for various control schemes. We see that the I&I (with adaptation on R only) and the PB estimators are slightly faster than

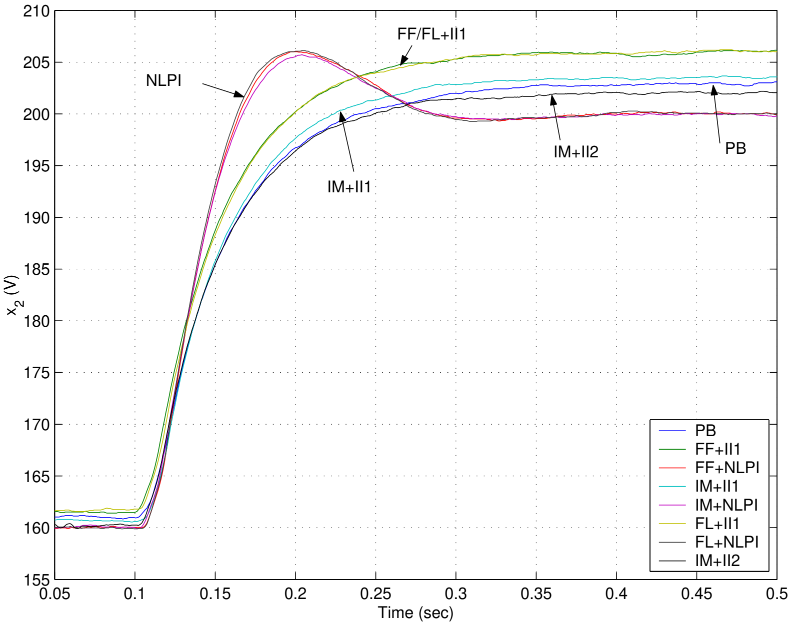

Figure 6: Response of the output voltage to a reference change from 160V to 200V applied at t=0.1s (the unknown parameter case).

the NLPI controller. However, there is a significant steady-state error, which changes when we perturb the load. This is mostly due to the uncertainty of the parameter r and to unmodeled dynamics. Applying the I&I adaptation on both R and r partially compensates for this uncertainty. However, the adaptation on r increases the third-order harmonics.

Table 4 shows the harmonic characteristics for each case. Again we see that the NLPI controller leads to the smallest steady-state error and, in combination with the FL control scheme, achieves the highest power factor. Figure 9 shows the input current, output voltage and the estimated parameter I_d for the FL+NLPI case.

Control	Error(V)	$\phi(^o)$	THD(%)	Power factor
PB	8.00	1.76	5.40	0.9981
FF+II$_1$	14.36	2.33	5.50	0.9977
FF+NLPI	0.04	2.81	5.74	0.9972
IM+II$_1$	5.56	1.92	5.73	0.9978
IM+NLPI	0.04	2.17	6.18	0.9974
FL+II$_1$	14.63	0.00	6.30	0.9980
FL+NLPI	0.04	0.55	6.12	0.9981
IM+II$_2$	0.95	1.65	7.11	0.9971

Table 4: Harmonic analysis results for $R = 51\Omega$.

Finally, Figure 10 shows the harmonic content of the input current for the IM+II$_2$ case compared to the european standard EN61000-3-2, which specifies the harmonic limits for equipment drawing up to 16A per phase. We conclude that all controllers proposed here achieve with a large margin the requirements imposed by this standard.

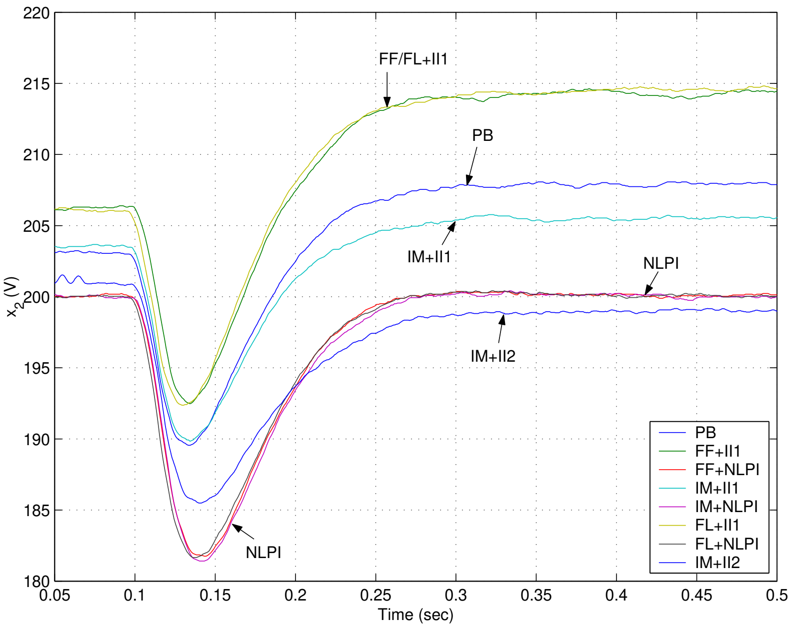

Figure 7: Response of the output voltage to a load change from 87Ω to 51Ω applied at t=0.1s (the unknown parameter case).

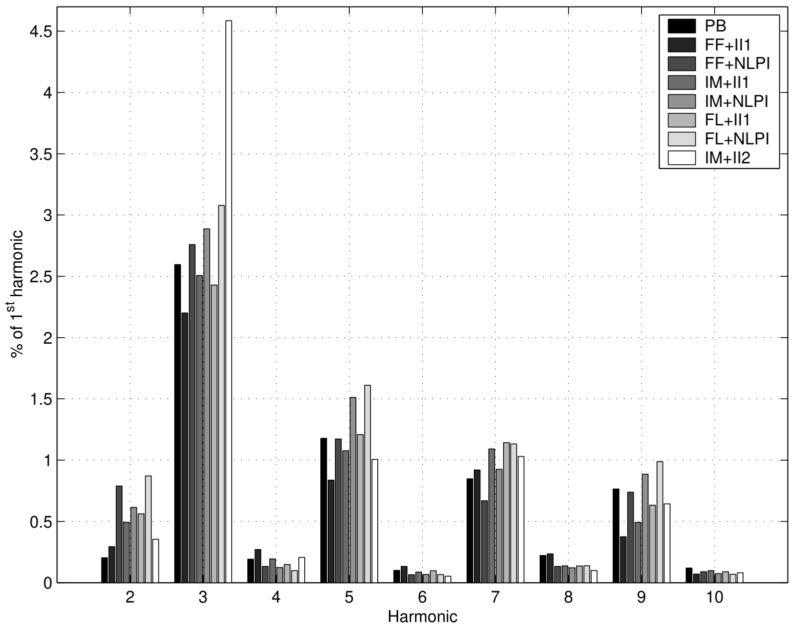

Figure 8: Amplitude of the input current harmonics for $R = 51\Omega$.

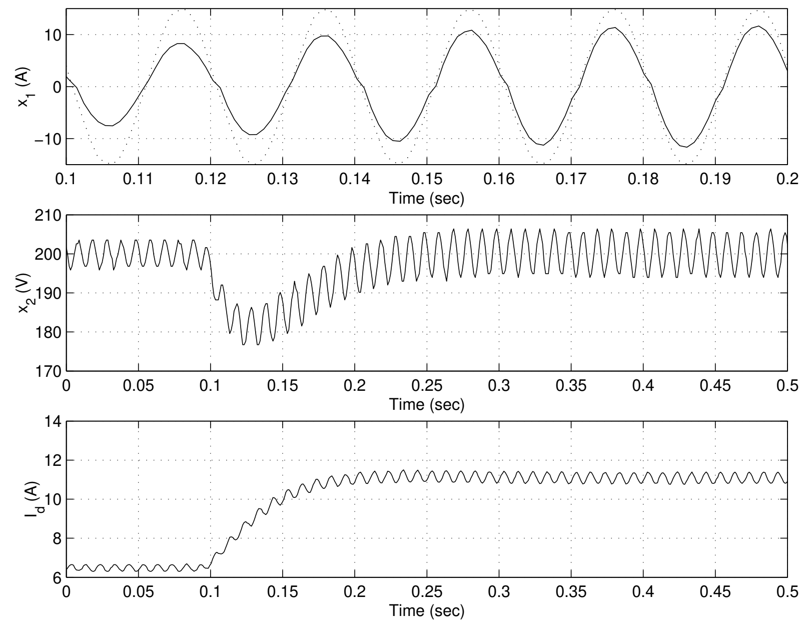

Figure 9: Response to a load change for the FL+NLPI controller. Top graph: input current (solid line) and input voltage (dotted line). Middle graph: output voltage. Bottom graph: estimated parameter I_d.

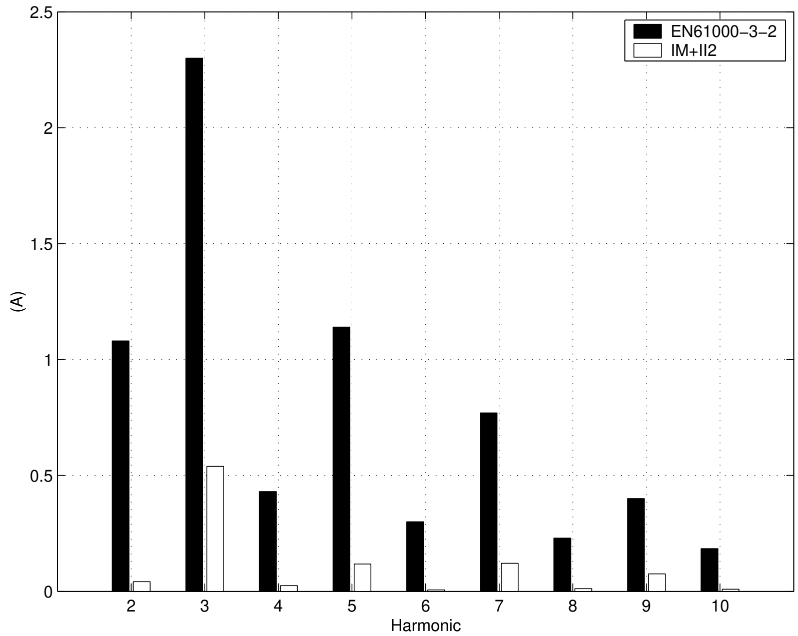

Figure 10: Amplitude of the input current harmonics for the IM+II$_2$ controller compared to the standard EN61000-3-2 (the amplitude of the first harmonic is 12A).

5 Conclusions

In this paper, an experimental comparison of several control schemes for a PFP circuit has been proposed. The results have shown that when the load R is known, the PB controller achieves the highest performance and robustness. If R is unknown and an adaptation mechanism on R is employed, the PB and IM control schemes are the most robust against changes in the load, at the expense of higher complexity. To further improve robustness, it is necessary to make use of a different adaptation scheme. Namely, it is necessary to adapt the parameter I_d. If such an adaptation is used, the FF, IM and FL controllers are (in steady state) almost insensitive to load changes. However, the transient response is slightly degraded. Finally, the FL control scheme is the easiest to implement, since it uses only static feedback and does not require the derivative of $x_1^\star(t)$. The trade-off is slightly higher harmonics and a small negative phase shift of the input current.[9] Further study is in progress to extend the proposed methodologies to more complex converters.

References

[1] A. Astolfi and R. Ortega. Immersion and invariance: a new tool for stabilization and adaptive control of nonlinear systems. In *IFAC Symposium on Nonlinear Control System Design, St. Petersburg, Russia*, pages 81–86, 2001.

[2] G. Escobar, D. Chevreau, R. Ortega, and E. Mendes. An adaptive passivity-based controller for a unity power factor rectifier. *IEEE Transactions on Control Systems Technology*, 9:637–644, 2001.

[3] J. G. Kassakian, M. F. Schlecht, and G. C. Verghese. *Principles of power electronics.* Addison-Wesley, 1991.

[4] N. Mohan, T. A. Undeland, and W. P. Robbins. *Power electronics: converters, applications and design.* John Wiley and Sons, 1995.

[5] R. Morici, C. Rossi, and A. Tonielli. Variable structure controller for AC/DC boost converter. In *20th International Conference on Industrial Electronics, Control and Instrumentation*, pages 1449–1454, 1994.

[6] R. Ortega and A. Astolfi. Nonlinear PI control of uncertain systems: an alternative to parameter adaptation. In *40th Conference on Decision and Control*, pages 1749–1754, 2001.

[9] However, as noted in Section 4.1, this last property may actually improve the power factor.